

A Survivor in the Era of Large-Scale Pretraining: An Empirical Study of One-Stage Referring Expression Comprehension

Gen Luo, Yiyi Zhou*, *Member, IEEE*, Jiamu Sun, Xiaoshuai Sun, *Member, IEEE*, Rongrong Ji, *Senior Member, IEEE*

Abstract—One-stage Referring Expression Comprehension (REC) is a task that requires accurate alignment between text descriptions and visual content. In recent years, numerous efforts have been devoted to cross-modal learning for REC, while the influence of other factors in this task still lacks a systematic study. To fill this gap, we conduct an empirical study in this paper. Concretely, we ablate 42 candidate designs/settings based on a common REC framework, and these candidates cover the entire process of one-stage REC from network design to model training. Afterwards, we conduct over 100 experimental trials on three REC benchmark datasets. The extensive experimental results reveal the key factors that affect REC performance in addition to multi-modal fusion, e.g., multi-scale features and data augmentation. Based on these findings, we further propose a simple yet strong model called SimREC, which achieves new state-of-the-art performance on these benchmarks. In addition to these progresses, we also find that with much less training overhead and parameters, SimREC can achieve better performance than a set of large-scale pre-trained models, e.g., UNITER and VILLA, portraying the special role of REC in existing V&L research¹.

I. INTRODUCTION

Referring expression comprehension [1]–[5], also known as *visual grounding* [6]–[9], is a task of locating the target instance in an image based on the natural language expression. As an vision and language (V&L) task, REC is not limited to a fixed set of object categories and can theoretically perform any open-ended detection according to text descriptions [1]. These appealing properties enable REC to garner widespread attention from the communities of both computer vision (CV) and vision and language (V&L) [1]–[4].

Due to the obvious advantage in efficiency, one-stage modeling has recently become the main research focus in REC [1], [2], [7]–[9]. Compared with the two-stage methods [3], [5], [6], [11], [12], one-stage models can omit the generation of region proposals and directly output the bounding box of the referent without complex image-text ranking, thereby improving the inference speed by an order of magnitude, as shown in Fig. 1. However, one-stage models often have worse

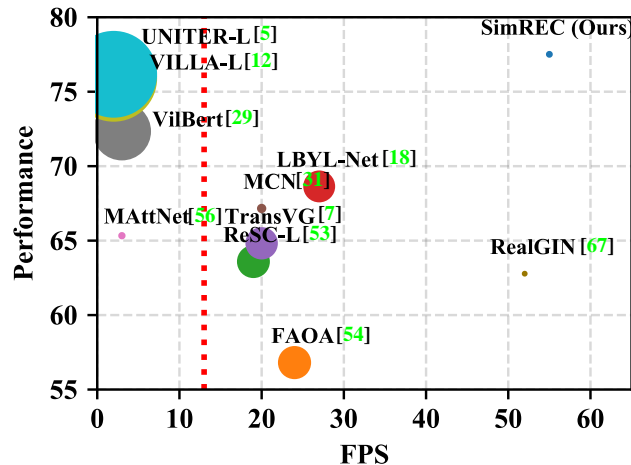


Fig. 1: Comparison of performance and inference speed between SimREC and other REC methods on the *val* set of RefCOCO+ [10]. The point size corresponds to the number of parameters. FPS denotes frames per second. Methods on the left side of the red line are two-stage, while the rest are one-stage.

performance than the two-stage ones [1], [2], [7]. Practitioners mainly attribute this shortcoming to the lack of enough multi-modal reasoning ability [1], [8], [9], [13]. To this end, recent endeavors put numerous efforts into the design of the multi-modal networks for one-stage REC, which have achieved notable success.

Despite these advances, the existing literature still lacks a systematic study to gain insight into one-stage REC. Differing from other V&L tasks, one-stage REC not only needs to realize the joint understanding of two modalities, but also requires very accurate language-vision alignments, *i.e.*, locating the referents with bounding boxes. Therefore, in addition to multi-modal fusion, other important factors also need to be further investigated, such as visual backbone, detection head and training paradigm. In this paper, we are committed to filling this research gap. We aim to figure out *what also matter in one-stage REC*, and *how they affect the REC performance*. Meanwhile, we also question that

whether REC, as an important V&L task, can be a survivor in the era dominated by large-scale BERT-style pre-trained models?

To approach these targets, we first build a common one-stage REC network framework, as shown Fig. 2. Based on this

G. Luo, Y. Zhou, J. Sun, X. Sun and R. Ji are with the Key Laboratory of Multimedia Trusted Perception and Efficient Computing, Ministry of Education of China, Xiamen University, 361005, P.R. China. G. Luo and R. Ji are also with the Peng Cheng Laboratory, Shenzhen 518000, China. (e-mail: luogen@stu.xmu.edu.cn, zhoyiyi@xmu.edu.cn, sunjiamu@stu.xmu.edu.cn, xssun@xmu.edu.cn, rrji@xmu.edu.cn).

*Corresponding Author: Yiyi Zhou (E-mail: zhoyiyi@xmu.edu.cn)

¹Source codes have been released at: <https://github.com/luogen1996/SimREC>.

framework, we conduct an empirical research that ablates 42 candidate designs / settings, which cover the most components of one-stage REC, such as visual backbone, language encoder, detection head and training paradigm *et al.* Afterwards, we conduct over 100 experimental trials on three benchmark datasets, namely RefCOCO [10], RefCOCO+ [10] and RefCOCOg [14], to examine the effects of these candidates. Lastly, these results constitute the main analysis data of this research.

This study yields significant findings for one-stage REC. Above all, it reflects the key factors that affect performance. Visual backbone and multi-scale visual features are critical for REC performance. And data augmentation, including image augmentation methods [15]–[18] and additional data [19], is also very beneficial. Meanwhile, we obtain some findings against the conventional impressions about REC. For example, REC is less affected by language bias, which is however very common in other V&L tasks like visual question answering [20]–[22]. In addition, we also notice that although some candidate designs obtain the expected performance gains, their practical use is still different to that in other tasks, *e.g.*, augmentation methods [15]–[18]. Detailed discussions are given in the experimental section.

By adopting these empirical findings, we further propose a simple yet strong model called SimREC, which outperforms most existing one-stage and two-stage methods in both accuracy and inference speed, as shown in Fig. 1. More importantly, with less training overhead and parameters, SimREC can achieve better performance than a bunch of large-scale pre-trained models [23]–[26], *e.g.*, VILLA-Large [25], on all benchmark datasets. We believe this result can be very enlightening for the existing V&L research, where the most tasks are dominated by the expensive large-scale models.

Overall, the contributions of this paper are three-fold:

- We present the first systematic study for one-stage REC, yielding several key factors in addition to multi-modal fusion.
- We propose a strong and simple model called SimREC, which outperforms a set of REC methods and large-scale pre-trained models in both performance and efficiency.
- We build a comprehensive and easy-to-use codebase² based on the content of this paper, which can greatly promote the development of one-stage REC.

II. RELATED WORK

Referring Expression Comprehension (REC) [1], [2], [5], [8], [22], [27]–[39] is a task to locate the referent based on a natural language expression. Early works [5], [27], [29]–[31], [33], [34], [40] often follow a two-stage pipeline. Concretely, two-stage models first detect the salient regions of an image, and then regard REC task as region-expression ranking problem. Despite the great success, these two-stage methods have obvious defects in model efficiency and generalization [7], [41].

²Our codebase is lightweight, extendable and general, and new REC models can be developed with minimal efforts. It also supports large-scale pre-training and multi-task learning of REC and RES on six common datasets, which is valuable for existing RES and REC researches.

To this end, one-stage REC has recently become a popular research direction [1], [2], [4], [7], [8], [13], [41]–[45]. By omitting the steps of region detection and image-text matching in multi-stage modeling, one-stage models greatly reduce the inference time, *e.g.*, 28.6 images per second, as reported in [1]. However, one-stage models often have worse REC performance compared with the two-stage methods, like MattNet [3], mainly due to the limited reasoning ability. In this case, recent advances are dedicated to improving the reasoning ability of one-stage REC and propose various novel multi-modal networks for one-stage REC [1], [8], [9], [13], [38], [40]. In particular, ReSC [8] proposes a multi-round reasoning module to handle long and complex expressions. LBYL [13] proposes a novel landmark feature convolution to better align the vision and language features. TransVG [9] improves multi-modal fusions via stacking multi-layer transformer blocks [46]. More recently, researchers have formulated REC as a sequence prediction task and proposed a set of novel sequence-to-sequence frameworks [42], [47]. For example, SeqTR [42] represents the bounding box of the referent with a sequence of discrete coordinate tokens, which are predicted via a Transformer architecture. In addition to the design of the network architecture, numerous efforts are devoted into multi-task learning [2], [42], [47]–[50], and greatly improve the upper bound of REC models. Despite the effectiveness, except the well studied multi-modal fusion, there still lacks a systematic study to examine the key components in one-stage REC.

Driven by the progresses of large-scale V&L pre-training, the new SOTA performance of REC is achieved by recent large-scale pre-training models [23]–[26], [51]. Specifically, these models are pre-trained with millions of image-text examples and excessive parameters, thereby dominating various downstream VL tasks, *e.g.*, VQA [20] and multi-modal retrieval [52]. In particular, common pre-training objectives of early VL pre-training are masked language modeling [24], [53] and image-text matching [23], [24]. When transferring to REC task, most of these models follow the two-stage paradigm and regard this task as a text and image region matching problem [23]–[26]. Nevertheless, these BERT-style pre-trained models are often defective in their expensive training costs and slow inference speed. Meanwhile, their pre-training objectives are also inefficient for the adaptation to REC task. In this paper, we are keen to find out whether a simple and efficient one-stage model can outperform these expensive pre-trained models.

III. THE FRAMEWORK AND ABLATION DESIGNS

To accomplish the empirical study, we first build a common one-stage REC framework, as depicted in Fig. 2. Then, we prepare a set of ablation designs and settings to examine the impact of different components.

A. Framework

Specifically, given an image I and an expression E , an one-stage REC model often uses a visual backbone and a language encoder to extract the visual and text features,

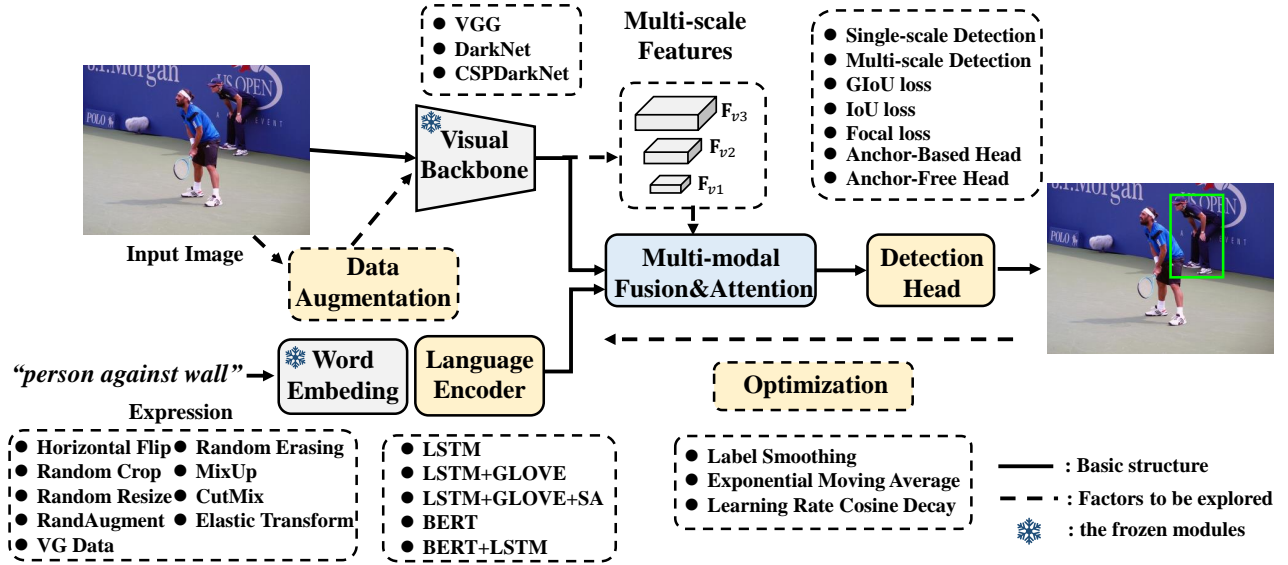


Fig. 2: The model framework and candidate designs/settings. The solid lines depict the basic structure. The dashed parts list candidate designs for the empirical study, which are used to examine the effects of different components in one-stage REC. The visual backbone and word embeddings are frozen during training.

denoted as $\mathbf{F}_v \in \mathbb{R}^{h \times w \times d}$ and $\mathbf{F}_t \in \mathbb{R}^{l \times d}$, respectively. Here, $h \times w$ denotes the resolution of visual feature maps, and l is the length of the expression. Here, the text features \mathbf{F}_t are attentively pooled [54] to a global vector $f_t \in \mathbb{R}^d$. Afterwards, a simple multi-modal fusion module is deployed to obtain the joint representations of two modalities, denoted as $\mathbf{F}_m \in \mathbb{R}^{h \times w \times d}$, which is obtained by:

$$f_m = \sigma(f_v \mathbf{W}_v) \odot \sigma(f_t \mathbf{W}_t). \quad (1)$$

Here, f_m and f_v are the feature vectors of \mathbf{F}_m and \mathbf{F}_v , respectively, and σ denotes the ReLU [55] activation function. To keep a certain reasoning ability, we also apply an attention unit called GARAN [1] after the multi-modal fusion.

Lastly, a regression layer is deployed to predict the bounding box of the referent in the image. Specifically, for each grid (g_x, g_y) , SimREC predicts raw coordinates of the bounding box $\{t_x, t_y, t_w, t_h\}$ and its corresponding confidence score c . Afterwards, the final bounding box $b = \{b_x, b_y, b_w, b_h\}$ is calculated based on the pre-defined anchor box (p_w, p_h) by

$$\begin{aligned} b_x &= \text{sigmoid}(t_x) + g_x, \\ b_y &= \text{sigmoid}(t_y) + g_y, \\ b_w &= p_w^{e^{t_w}}, b_h = p_h^{e^{t_h}}. \end{aligned} \quad (2)$$

Given the ground-truth box $b' = \{b'_x, b'_y, b'_w, b'_h\}$ and the ground-truth confidence c' , the loss function of SimREC is defined as:

$$l(b_i, b'_i, c_i, c'_i) = \sum_{i=1}^{h \times w \times n} c'_i * l_{box}(b_i, b'_i) + l_{conf}(c'_i, c_i) \quad (3)$$

Here, n is the number of pre-defined anchor boxes. l_{box} and l_{conf} denote the regression loss and the binary prediction loss of the confidence score, respectively. During the test stage, SimREC will select the bounding box with the highest confidence score as the final prediction.

Although the framework is simple, it includes the main design patterns of most existing one-stage REC models, *i.e.*, image encoder, language encoder, fusion branch and detection head. Meanwhile, a simple framework can be used to better examine other key factors for one-stage REC in addition to multi-modal fusion. With this simple framework, we can better ablate the key factors in one-stage REC.

B. Ablation Designs

Visual Backbone. We use DarkNet [56] as the default visual backbone. VGG [57] and the recently proposed CSPDarkNet [58] are the candidate choices. Meanwhile, we also test the effects of different image resolutions.

Language Encoder. The default language model is an LSTM network [59] with GLOVE embeddings [60]. During experiments, we will enhance the ability of language encoder by adding advance designs like self-attention [46] and BERT embedding [53].

Multi-scale Features and Detection. We also experiment the model with multi-scale features and multi-scale detection setting. In terms of multi-scale features, we use the last k scale feature maps of the visual backbone as our visual features, denoted as $\{\mathbf{F}_{vi}\}_{i=1}^k$. The features of each scale are fused with the text ones by the multi-scale fusion scheme proposed in [2], denoted as $\{\mathbf{F}_{mi}\}_{i=1}^k$. Only the last scale feature maps are used, *i.e.*, \mathbf{F}_{mk} . In terms of multi-scale detection, each scale feature in $\{\mathbf{F}_{mi}\}_{i=1}^k$ will use a corresponding detection head to predict bounding boxes.

Detection Paradigms. In addition to the anchor-based detection head [56], we also experiment the recently popular anchor-free detection [61]. In anchor-free detection, the model directly predict the width and height of bounding boxes for each grid. The objectives we test include *IoU* loss [62], *GloU* loss [62], *Smooth-L1* loss [63] and *Focal* loss [64].

Data Augmentation. We adopt additional data, *i.e.*, Visual Genome [19], and image augmentation methods [15]–[18], [65] for data augmentation. In terms of image augmentation, we try *ElasticTransform*, *CutMix* [17], *Random Resize*, *RandomAugment* [16] and *MixUp* [65]. Their detailed modification for REC are described in our appendix.

Optimizations. To regularize and accelerate the model training, we also examine some training techniques, *e.g.*, label smoothing [66], exponential moving average (EMA) [67] and cosine decay learning schedule [66].

C. SimREC

After the extensive ablations, we select the most effective designs for each REC component to form our strong base model, denoted as *SimREC*. The detailed configurations are listed in Tab. I.

IV. EXPERIMENTS

A. Datasets and Metric

RefCOCO & RefCOCO+ [10] contain 142k referring expressions for 50k bounding boxes in 19k images from MS-COCO [52]. There are four splits in RefCOCO and RefCOCO+, *i.e.*, *train*, *val*, *testA* and *testB*, with a number of 12k, 10k, 5k, 5k images, respectively. Test A contains more *people* instances, while Test B has more *object* ones. The expressions of RefCOCO are mainly about absolute spatial relationships, while the ones of RefCOCO+ are about attributes and relative relations. **RefCOCOg** [14], [74] has 104k expressions for 54k objects from 26k images. It has two different partitions, *i.e.*, *Google* split [74] and *UMD* split [14]. *Google* split only contains training set and validation set, and images of which are overlapped. Instead, *UMD* split avoids overlapping partitions, and it contains three splits, *i.e.*, *train*, *validation* and *test*. In particular, the expressions of RefCOCOg are longer and more complex than those of RefCOCO and RefCOCO+. **Visual Genome** [19] contains 5.6M referring expressions for 101K images. Compared to RefCOCO, RefCOCO+ and RefCOCOg, the expressions of Visual Genome are more diverse but their annotations are relatively noisy.

Intersection-over-Union (IoU) is the metric used in REC, which measures the overlap degree between the prediction and the ground-truth. Following previous works [1], [2], [7], [8], we use *IoU@0.5* to measure prediction accuracy.

B. Experimental Settings

Network Configurations. The visual backbone and the language encoder of SimREC are a CSPDarknet [58] and an LSTM [59] with a self-attention layer [46], respectively. For SimREC, we use three-scale visual features from the visual backbone outputs of stride=8, stride=16 and stride=32, of which dimensions are 256, 512, 1024, respectively. For language encoder, its dimension is set to 512 and the word embedding is a 300-d matrix initialized by pre-trained GLOVE vectors [60]. By default, the input image is resized to 416×416 , and the maximum length of input expressions is set to 15

for RefCOCO and RefCOCO+, and 20 for RefCOCOg. For detection head and loss function, we apply the anchor-free head [61] with IoU loss [62] and BCE loss. For data augmentations, random resize is used in the training. To improve the training efficiency, we further apply the exponential moving average (EMA) [67] and cosine decay learning schedule.

Training settings. We use Adam [75] to train our models for 40 epochs, which can be reduced to 25 epochs when EMA is applied. The learning rate is initialized with $1e-4$ and will be decayed by 10 at the 35-th, 37-th and 39-th epoch, respectively. We also try the cosine decay as the learning rate schedule. All visual backbones are pre-trained on MS-COCO [52], while the images appeared in the val and test sets of three REC datasets are removed. We also apply the region annotations in the Visual Genome [76] to pre-train SimREC. Particularly, pre-trained stage takes 15 epochs with a batch size of 256. The learning rate and optimization are kept the default settings.

C. Experimental Results

1) *Ablation Study:* We first conduct extensive experiments on benchmark datasets to ablate the candidate designs/settings described in Sec. IV-C1, of which results are shown in Tab. I. **What matters in one-stage REC?** From Tab. I, we first observe that the visual components are critical for one-stage REC. The use of a better backbone or detection head can lead to significant performance gains. In particular, Swin-Transformer [68] provides the most significant gains, *i.e.*, +9.6% on RefCOCO+. Nevertheless, such a large visual backbone also slows down the inference speed of the one-stage REC model. In contrast, anchor-free head not only boosts the detection performance but also maintains the inference efficiency. Meanwhile, larger image resolutions are also more beneficial for performance. These results are within the scope of existing CV and V&L studies [56], [63], [77]–[79].

Multi-scale visual features are the factor that can boost performance. On RefCOCO+, its performance gain can reach up to +14.3%, while the ones on the other two datasets are also about +6%. However, when combining it with multi-scale detection, the performance is not further improved. This result suggests that multi-scale features are basically used to enhance the descriptive power of visual backbones rather than multi-scale detection, which is obviously different to the use in object detection [56], [63].

Data augmentation is another factor that greatly affects performance. Using Visual Genome (VG) as the additional training data can greatly boost performance on all benchmarks. Meanwhile, a simple image augmentation like *Resizing* also obtain obvious performance gains. These results suggest that one-stage REC has a great demand in training data, especially compared with other V&L tasks [20], [21]. For example, VG is often used as additional data in VQA, while the improvement is often marginal [54], [80]. From Tab. I, we can also summarize a prerequisite for data augmentation, which is that the semantics of image-text pairs should not be damaged. The operations like *Horizontal Flip* and *Random Crop* will reduce the completeness or the correctness of REC examples, thus leading to counterproductive results. Meanwhile, strong

TABLE I: Ablation studies of different factors on three REC datasets. † denotes the settings of the basic structure and ‡ denotes the settings of SimREC. “DN53”, “CDN53”, “Swin-B” and “ViT-B” refer to the visual backbone of DarkNet-53 [56], CSPDarkNet-53 [61], Swin-Transformer (Base) [68] and Vision Transformer (Base) [69], respectively. For all the results, we average three experimental results of different random seeds.

Factors	Choices	RefCOCO val		RefCOCO+ val		RefCOCOg val		Inference Speed ⁴		Training Time	
		Acc	Δ	Acc	Δ	Acc	Δ	FPS	Δ	Hours	Δ
Visual Backbone	DN53†	70.63	+0.00	50.39	+0.00	58.78	+0.00	59.2	+0.0	6.6 h	+0.0h
	VGG16	70.12	-0.51	49.81	-0.58	58.22	-0.56	46.9	-12.3	9.9 h	+3.3h
	CDN53‡	71.90	+1.17	57.24	+6.85	57.58	-1.20	74.1	+14.9	5.4 h	-1.2h
	ViT-B	72.60	1.97	58.12	+7.73	60.19	+1.41	30.6	-28.6	10.1h	+3.5h
	Swin-B	75.10	+4.47	59.96	+9.57	62.03	+3.25	36.2	-23.0	9.7h	+3.1h
Language Encoder	LSTM+GLOVE†	70.63	+0.00	50.39	+0.00	58.78	+0.00	59.2	+0.0	6.6 h	+0.0h
	LSTM	70.06	-0.57	49.54	-0.85	57.78	-1.00	59.2	+0.0	6.6 h	+0.0h
	LSTM+GLOVE+SA(1)‡	71.56	+0.93	51.26	+0.87	58.11	-0.67	58.1	-1.1	6.7 h	+0.1h
	LSTM+GLOVE+SA(2)	71.17	+0.54	50.65	+0.26	58.42	-0.36	57.1	-2.1	6.7 h	+0.1h
	LSTM+GLOVE+SA(3)	71.43	+0.80	48.73	-1.66	59.15	+0.37	55.9	-3.3	6.7 h	+0.1h
	LSTM+BERT	70.66	+0.03	50.27	-0.12	60.31	+1.53	42.0	-17.2	7.8 h	+1.2h
	LSTM+RoBERTa	70.84	+0.21	50.44	-0.05	60.56	+1.78	41.3	-17.9	7.9 h	+1.3h
	LSTM+ALBERT	71.44	+0.81	50.76	+0.37	60.44	+1.66	51.1	-8.1	7.4 h	+0.6h
Multi-scale Features	One-scale Feature†	70.63	+0.00	50.39	+0.00	58.78	+0.00	59.2	+0.0	6.6 h	+0.0h
	Two-scale Features	76.79	+6.16	63.71	+13.32	62.62	+3.84	54.1	-5.1	7.9 h	+1.3h
	Three-scale Features‡	77.41	+6.78	64.72	+14.33	65.51	+6.73	49.0	-10.2	10.8 h	+4.2h
	Four-scale Features	78.33	+7.70	65.21	+14.82	65.56	+6.78	42.9	-16.3	11.1 h	+4.5h
Multi-scale Detection	One-scale Feature+Head×1†	70.63	+0.00	50.39	+0.00	58.78	+0.00	59.2	+0.0	6.6 h	+0.0h
	Three-scale Features+Head×1‡	77.41	+6.78	64.72	+14.33	65.51	+6.73	49.0	-10.2	10.8 h	+4.2h
	Three-scale Features+Head×3	77.40	+6.77	62.78	+12.39	64.73	+5.95	39.2	-20.0	14.5 h	+7.9h
Detection Head	Anchor-Based†	70.63	+0.00	50.39	+0.00	58.78	+0.00	59.2	+0.0	6.6 h	+0.0h
	Anchor-Free‡	73.65	+3.02	53.49	+3.10	59.46	+0.68	55.9	-3.3	9.1 h	+2.5h
Loss Fuction	BCE+MSE†	70.63	+0.00	50.39	+0.00	58.78	+0.00	59.2	+0.0	6.6 h	+0.0h
	Focal loss+MSE	70.43	-0.20	49.86	-0.53	58.42	-0.36	59.2	+0.0	6.7 h	+0.1h
	BCE+SmoothL1	71.12	+0.49	50.29	-0.10	59.23	+0.45	59.2	+0.0	6.7 h	+0.1h
	BCE+IoU loss‡	71.39	+0.76	51.68	+1.29	59.54	+0.76	59.2	+0.0	6.7 h	+0.1h
	BCE+GIoU loss	70.76	+0.13	50.34	-0.05	59.42	+0.64	59.2	+0.0	6.7 h	+0.1h
	Reward loss ³	69.77	-0.86	50.89	+0.60	60.10	+1.32	15.6	-43.6	17.2h	+10.5
Input Resolution	416 × 416 † ‡	70.63	+0.00	50.39	+0.00	58.78	+0.00	59.2	+0.0	6.6 h	+0.0h
	256 × 256	64.57	-6.06	47.25	-3.14	52.63	-6.15	69.0	+9.8	3.6 h	-3.0h
	320 × 320	68.53	-2.10	49.13	-1.26	56.86	-1.92	67.1	+7.9	5.0 h	-1.6h
	512 × 512	70.97	+0.34	51.28	+0.89	59.97	+1.19	46.9	-12.3	9.6 h	+3.0h
	608 × 608	71.15	+0.52	51.59	+1.20	59.38	+0.60	41.0	-18.2	12.6 h	+6.0h
Data Augmentations	None†	70.63	+0.00	50.39	+0.00	58.78	+0.00	59.2	+0.0	6.6 h	+0.0h
	Horizontal Flip	66.58	-4.05	47.92	-2.47	56.13	-2.65	59.2	+0.0	6.6 h	+0.0h
	Random Crop	61.20	-9.43	47.06	-3.33	51.67	-7.11	59.2	+0.0	6.8 h	+0.2h
	Elastic Transform	71.91	+1.28	52.36	+1.97	60.58	+1.80	59.2	+0.0	6.7 h	+0.1h
	Random Resize‡	74.07	+3.44	55.61	+5.22	62.79	+4.01	59.2	+0.0	7.8 h	+1.2h
	RandAugment	72.89	+2.26	53.23	+2.84	61.85	+3.07	59.2	+0.0	7.6 h	+1.0h
	Random Erasing	71.29	+0.66	51.79	+1.40	59.62	+0.84	59.2	+0.0	7.4 h	+0.8h
	Mixup	72.63	+2.00	51.09	+0.70	59.56	+0.78	59.2	+0.0	7.2 h	+0.6h
	CutMix	72.42	+1.79	52.40	+2.01	60.42	+1.64	59.2	+0.0	7.2 h	+0.6h
	VG Data‡	78.23	+7.60	65.18	+14.79	70.40	+11.62	59.2	+0.0	118.3h	+111.7h
Optimizations	None†	70.63	+0.00	50.39	+0.00	58.78	+0.00	59.2	+0.0	6.6 h	+0.0h
	Label Smoothing	70.78	+0.15	50.93	+0.54	59.27	+0.49	59.2	+0.0	6.6 h	+0.0h
	Exponential Moving Average‡	71.95	+1.32	51.78	+1.39	60.46	+1.68	59.2	+0.0	5.1 h	-1.5h
	Learning Rate Cosine Decay‡	70.79	+0.16	50.63	+0.30	59.44	+0.66	59.2	+0.0	6.6 h	+0.0h

TABLE II: Results of combining different data augmentations.

Data Augmentations	RefCOCO (val)	
	Acc	Δ
Random Resize (Baseline)	74.07	+0.00
MixUp+CutMix	72.61	-1.46
RandAugment+Elastic Transform	71.99	-2.08
RandAugment+Random Resize	73.77	-1.00
MixUp+Random Resize	71.51	-2.56
All Useful Augmentations	66.08	-7.99

augmentation methods are inferior than the simple ones, e.g., RandomErasing and CutMix. When combing all positive augmentation methods, the REC performance encounters a significant decline, as shown in Tab. II, which is opposite to that in object detection [79]. These results greatly differ REC

from object detection in terms of data augmentation.

In Tab. III, we conduct cumulative ablations to validate the combination of SimREC settings. From the results, we observe that each factor consistently improves performance when combined with other factors. Particularly, multi-scale features and VG data augmentations still play the most critical role on performance, providing up to +12.94% gains on RefCOCOg test set. Meanwhile, the combination of other factors also brings notable performance gains. For example, language encoder, visual backbone, detection head, optimizations and random resize provide the improvements of +1.75%, +1.65%, +2.61%, +0.27% and +1.76% on RefCOCOg test set, respectively. And their combination finally improves the performance by +8.04% on RefCOCOg test set. After combining all factors, +20.98%

TABLE III: Cumulative Ablations of SimREC on three REC datasets. The basic structure adopts the default setting of TABLE I. Each row represents the performance after applying the setting of SimREC.

Models	Net #Params ⁵	RefCOCO			RefCOCO+			RefCOCog		Inference Speed ⁴									
		val	testA	testB	val	testA	testB	val	test										
Basic Structure	7M	70.63	+0.00	72.28	+0.00	66.50	+0.00	50.39	+0.00	52.93	+0.00	45.12	+0.00	58.78	+0.00	58.58	+0.00	58.8 fps	+0.0 fps
+ Three-scale Features	12M	77.41	+6.78	81.14	+8.86	71.85	+5.35	64.72	+14.33	69.09	+16.16	59.49	+14.37	65.51	+6.73	64.82	+6.24	50.0 fps	-8.8 fps
+ LSTM-GLOVE-SA(1)	16M	78.21	+7.58	81.22	+8.94	71.94	+5.44	64.83	+14.44	70.22	+17.29	55.23	+10.11	66.65	+7.87	66.57	+7.99	48.8 fps	-10.0 fps
+ Anchor-free Head	16M	79.74	+9.11	82.67	+10.39	73.56	+7.06	68.25	+17.86	73.12	+20.19	58.45	+13.33	69.22	+10.44	69.18	+10.60	47.9 fps	-10.9 fps
+ Optimizations	16M	80.88	+10.25	83.23	+10.95	75.22	+8.72	68.57	+18.18	73.65	+20.72	58.79	+13.67	69.26	+10.48	69.45	+10.87	47.9 fps	-10.9 fps
+ Random Resize	16M	82.03	+11.40	85.01	+12.73	77.65	+11.15	70.24	+19.85	75.87	+22.94	60.87	+15.75	71.43	+12.65	71.21	+12.63	47.9 fps	-10.9 fps
+ CSPDarknet	16M	82.45	+11.82	85.91	+13.63	77.98	+11.48	70.58	+20.19	76.75	+23.82	61.12	+16.00	72.59	+13.81	72.86	+14.28	55.6 fps	-3.2 fps
+ VG Data	16M	86.49	+15.86	88.95	+16.67	81.74	+15.24	77.51	+27.12	82.68	+29.75	68.81	+23.69	79.88	+21.10	79.56	+20.98	55.6 fps	-3.2 fps

TABLE IV: Comparison of SimREC and the state-of-the-arts on three REC datasets. SimREC (scratch) is not pre-trained on VG. TransVG+SimREC denotes that the findings of SimREC are applied to TransVG. † denotes that model is fine-tuned on the combination of three REC datasets. The result colored in gray denotes that the model is trained with multi-task supervised learning, which requires more labeled data. The numbers in bold denote the best performance, while the underlined numbers are the ones among the compared methods. All inference speeds are tested on an NVIDIA 1080Ti (11GB).

Models	Visual Features	Pretrain Images	Net #Params ⁵	RefCOCO			RefCOCO+			RefCOCog		Inference Speed ⁴
				val	testA	testB	val	testA	testB	val-u	test-u	
<i>Two-stage:</i>												
CMN [27] _{CVPR17}	VGG16	-	-	-	71.03	65.77	-	54.32	47.76	-	-	-
MAttNet [3] _{CVPR18}	RN101	-	18M	76.65	81.14	69.99	65.33	71.62	56.02	66.58	67.27	2.6 fps
NMTree [6] _{ICCV19}	RN101	-	-	76.41	81.21	70.09	66.46	72.02	57.52	65.87	66.44	-
CM-Att-Erase [12] _{CVPR19}	RN101	-	-	78.35	83.14	71.32	68.09	73.65	58.03	67.99	68.67	-
<i>One-stage:</i>												
RealGIN [1] _{TNNLS21}	DN53	-	12M	77.25	78.70	72.10	62.78	67.17	54.21	62.75	62.33	52.6 fps
FAOA [7] _{ICCV19}	DN53	-	120M	72.54	74.35	68.50	56.81	60.23	49.60	61.33	60.36	25.0 fps
ReSC [8] _{ECCV20}	DN53	-	120M	77.63	80.45	72.30	63.59	68.36	56.81	67.30	67.20	18.9 fps
MCN [2] _{CVPR20}	DN53	-	26M	80.08	82.29	74.98	67.16	72.86	57.31	66.46	66.01	20.3 fps
Iter-Shrinking [4] _{CVPR21}	RN101	-	-	-	74.27	68.10	-	71.05	58.25	-	70.05	-
PFCOS [36] _{TMM22}	DN53	-	-	79.50	81.49	77.13	65.76	69.61	60.30	69.06	68.34	-
LBYL-Net [13] _{CVPR21}	DN53	-	115M	79.67	82.91	74.15	68.64	73.38	59.49	-	-	27.0 fps
TransVG [9] _{ICCV21}	RN101	-	117M	81.02	82.72	78.35	64.82	70.70	56.94	68.67	67.73	19.6 fps
TransVG [9]+SimREC	CDN53	-	117M	82.23	85.24	79.85	68.52	73.42	60.11	70.03	69.88	27.5 fps
One-for-All [50] _{Neurocomputing23}	DN53	-	-	76.99	79.71	72.67	61.58	66.60	54.00	66.03	66.70	-
SeqTR [42] _{ECCV22}	DN53	-	19M	81.23	85.00	76.08	68.82	75.37	58.78	71.35	71.58	21.2 fps
PLV-FPN [43] _{TIP22}	RN101	-	-	81.93	84.99	76.25	71.20	77.40	61.08	70.45	71.08	-
Word2Pix [44] _{TNNLS22}	RN101	-	-	81.20	84.39	78.12	69.74	76.11	61.24	70.81	71.34	-
QRNet [45] _{CVPR22}	Swin-S	-	117.9M	<u>84.01</u>	<u>85.85</u>	<u>82.34</u>	<u>72.94</u>	<u>76.17</u>	<u>63.81</u>	<u>71.89</u>	<u>73.03</u>	20.1 fps
SimREC (ours)	DN53	-	16M	82.03	85.01	77.65	70.24	75.39	61.85	71.43	72.07	50.0 fps
SimREC (ours)	CDN53	-	16M	82.45	85.91	77.98	70.58	76.75	61.12	72.59	72.86	55.6 fps
SimREC (ours)	Swin-B	-	16M	84.93	86.55	83.85	73.09	76.02	66.28	75.90	75.55	36.2 fps
<i>Additional REC data:</i>												
MDETR [51] _{ICCV21}	RN101	0.2M	143M	86.75	89.58	81.41	<u>79.52</u>	<u>84.09</u>	<u>70.62</u>	<u>81.64</u>	<u>80.89</u>	<u>15.4 fps</u>
UniTAB [70] _{ECCV22}	RN101	0.2M	-	86.32	88.84	80.61	78.70	83.22	69.48	79.96	79.97	-
SeqTR [42] _{ECCV22}	DN53	0.2M	19M	87.00	90.15	83.59	78.69	84.51	71.87	82.69	83.37	21.2 fps
UNINEXT† [48] _{CVPR23}	RN50	0.6M	-	89.72	91.52	86.93	79.76	85.23	72.78	83.95	84.31	-
PolyFormer-L† [47] _{CVPR23}	Swin-L	0.2M	363M	90.38	92.89	87.16	84.98	89.77	77.97	85.83	85.91	2.5 fps
SimREC	Swin-B	0.2M	16M	88.80	89.48	87.58	78.94	82.69	72.80	82.84	83.41	30.6 fps
SimREC	CDN53	0.2M	16M	88.47	90.75	84.10	80.25	85.33	72.04	83.08	83.99	55.6 fps
SimREC†	CDN53	0.2M	16M	89.39	92.12	86.06	81.42	86.74	74.13	83.64	85.02	55.6 fps

performance gains can be observed on RefCOCog *test* set. These results further confirm the effectiveness of SimREC.

What are less important in one-stage REC? Compared with the above mentioned factors, the other components have less impact on one-stage REC. Above all, the role of language encoder is not as important as that in other V&L tasks. By deploying the advanced designs like BERT [53] and ALBERT [81], the performance gains are not obvious. Even on RefCOCog, of which expressions are long and complex, the improvement is only +1.78%. One assumption about this result

is that the expressions of REC is not so difficult to understand. But more importantly, it may also suggest that REC is less affected by language priors, which is often serious in other V&L tasks [20], [21], [82]. In this case, a simple design can meet the requirement of expression comprehension.

In Tab. I, we evaluate the effects of different loss functions and training tricks. The loss functions are deployed on the anchor-based detector [56], while their performance gains are not obvious, especially compared with object detection [62]. This results may suggest that pre-defined anchors are not suitable for one-stage REC. We also validate the effect of the reinforcement learning approach [4], which reduces the per-

³Reward loss is borrowed from Iter-Shrinking [4], which requires multiple forwards during inference.

TABLE V: Comparison of SimREC and large-scale BERT-style pre-trained models on three REC datasets. ‡ denotes that model is fine-tuned on the combination of three REC datasets. The result colored in gray denotes that the model uses much more labeled data.

Models	Visual Features	Pretrain Images	Net #Params ⁵	RefCOCO			RefCOCO+			RefCOCOg		Inference Speed ⁴
				val	testA	testB	val	testA	testB	val-u	test-u	
ViiBERT [23] _{NeurIPS19}	RN101	3.3M	221M	-	-	-	72.34	78.52	62.61	-	-	2.5 fps
ERNIE-ViL-L [26] _{AAAI21}	RN101	4.3M	-	-	-	-	75.89	82.37	66.91	-	-	-
UNITER-L [24] _{ECCV20}	RN101	4.6M	335M	81.41	87.04	74.17	75.90	81.45	66.70	74.86	75.77	2.4 fps
VILLA-L [25] _{NeurIPS20}	RN101	4.6M	335M	<u>82.39</u>	<u>87.48</u>	<u>74.84</u>	<u>76.17</u>	<u>81.54</u>	66.84	<u>76.18</u>	<u>76.71</u>	2.4 fps
OFA-B‡ [49] _{ICML22}	RN101	60.6M	137M	88.48	90.67	83.30	81.39	87.15	74.29	82.29	82.31	9.7 fps
OFA-L‡ [49] _{ICML22}	RN152	60.6M	412M	90.05	92.93	85.26	85.80	89.87	79.22	85.89	86.55	2.7 fps
SimREC	DN53	0.1M	16M	85.72	88.10	81.28	76.11	81.57	66.49	77.78	78.28	50.0 fps
SimREC	CDN53	0.1M	16M	86.49	88.95	81.74	77.51	82.68	68.81	79.88	79.56	55.6 fps
SimREC	Swin-B	0.2M	16M	88.80	89.48	87.58	78.94	82.69	72.80	82.84	83.41	30.6 fps
SimREC	CDN53	0.2M	16M	88.47	90.75	84.10	80.25	85.33	72.04	83.08	83.99	55.6 fps
SimREC‡	CDN53	0.2M	16M	89.39	92.12	86.06	81.42	86.74	74.13	83.64	85.02	55.6 fps

TABLE VI: Comparison of SimREC and the state-of-the-arts on Referit and Flickr.

Models	Visual Features	Referit test	Flickr test
<i>Two-stage:</i>			
MAttNet [3]	RN101	29.04	-
Similarity Net [71]	RN101	34.54	60.89
DDPN [72]	RN101	63.00	73.30
<i>One-stage:</i>			
ZSGNet [73]	RN50	58.63	63.39
FAOA [7]	DN53	60.67	68.71
ReSC [8]	DN53	64.60	69.28
TransVG [9]	RN101	70.73	<u>79.10</u>
SimREC	CDN53	77.80	83.31

formance and the efficiency. In terms of model optimization, all candidate methods pose positive impacts on performance although not so obvious. Particularly, we find that EMA [67] can accelerate training convergence.

How do these factors affect REC? Based on the above findings, we further explore how these key factors affect one-stage REC. Specifically, we investigate their effects on expressions of different content and lengths in Fig. 3, and the quality of predicted bounding boxes in Fig. 4.

From Fig. 3, we can first observe that multi-scale features and data augmentations can improve the model performance on all expressions, especially the ones with attribute descriptions (words). In this regard, we think that multi-scale features are to enhance the visual representations to facilitate fine-grained recognition, while data augmentation can significantly strengthen the learning of language-vision alignments. These two aspects are critical for REC. In addition, we also notice that the improvement of the expressions with spatial information (words) is small. We attribute it to the intrinsic merit of one-stage REC modeling in spatial relation modeling [1]. Meanwhile, we can also find that with the improvement in visual modeling, the model also has a better ability to process the long and complex expressions, especially with the help of VG. This result also provides a useful hint for the study of multi-modal reasoning.

Compared with these two factors, the benefit of detection head is more balanced. For this end, we understand that detection head mainly affects the model’s detection ability.

TABLE VII: Results of applying our findings to Transformer-based REC model. ViLT is pre-trained on 3M image-text pairs. By default, we use the [cls] token to predict the box of the referent during fine-tuning.

RefCOCO			
	val	testA	testB
TransVG [9]	81.02	82.72	78.35
ViLT [83]	79.51	82.15	71.93
TransVG+SimREC	82.52	84.12	79.85
ViLT+SimREC	83.23	85.24	79.12
RefCOCO+			
	val	testA	testB
TransVG [9]	64.82	70.70	56.94
ViLT [83]	65.32	71.30	54.63
TransVG+SimREC	68.52	73.42	60.11
ViLT+SimREC	73.70	78.54	63.57
RefCOCOg			
	val	test	
TransVG [9]	68.67	67.73	
ViLT [83]	67.03	66.35	
TransVG [9]+SimREC	70.03	69.88	
ViLT+SimREC	73.53	74.05	

Besides, Fig. 3 also reflects the inference of language encoder, which is relatively small. Since most of the sentences in benchmark datasets are short, the help of language encoder is not obvious. In contrast, it also affects its performance on long sentences. This observation is consistent with the experimental results in Tab. I.

Fig. 4 depicts the IoU score distributions of the model’s predictions about the ground-truth bounding boxes. These results reflect the impact of these factors on the quality of model predictions. From this figure, we observe that the anchor-free detector obviously improves the detection ability. On the high-quality detection (IoU 0.9-1), the number is almost doubled by this detector. Meanwhile, we notice that the use of VG helps the model improve the detection accuracy (IoU>0.5), but its performance on high-quality detection declines obviously. This is mainly attributed to the less accurate bounding box annotations in VG [19].

2) *Comparison with the state-of-the-art methods:* After making trade-offs between performance and efficiency, we further combine some findings from Tab. I to strengthen our baseline network SimREC. The cumulative ablation results are given in Tab. III. Then, we compare SimREC to a set of state-of-the-art (SOTA) methods in REC.

⁴Inference speed is tested on the 1080Ti (11GB).

⁵The calculation of network parameters excludes the visual backbone.

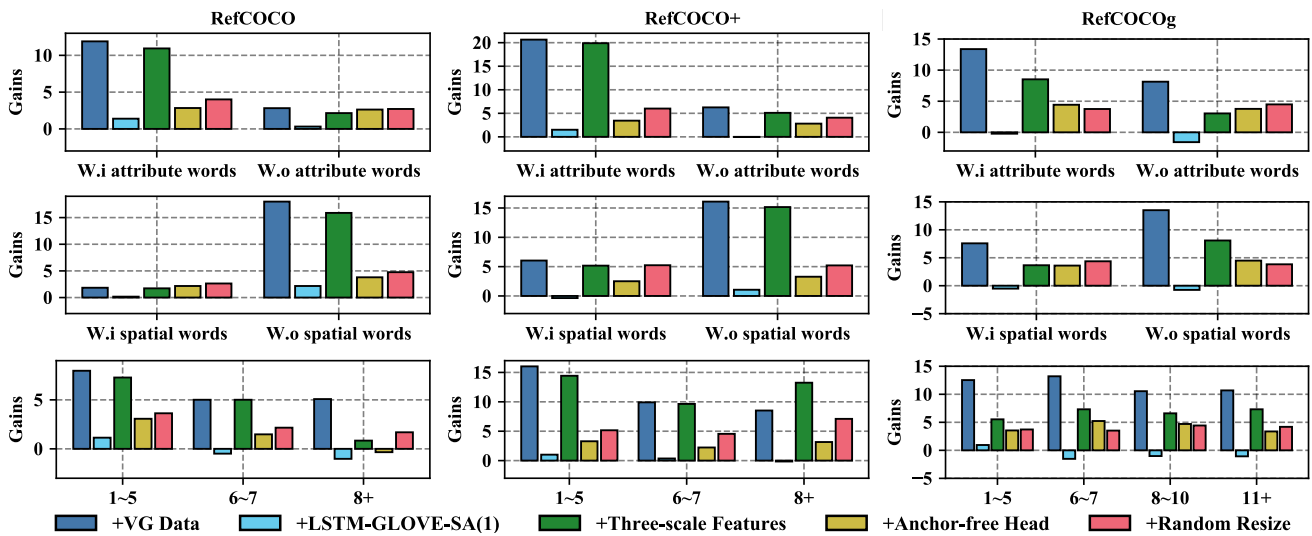


Fig. 3: Relative performance gains of five settings in SimREC on attribute descriptions (row-1), spatial descriptions (row-2), the expression length (row-3). All results are calculated on the *val* set.

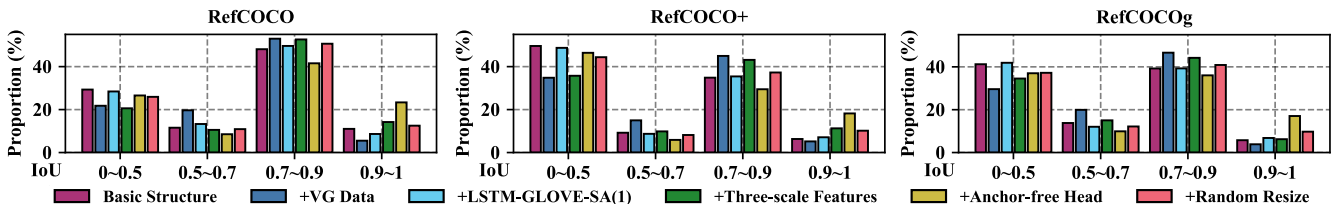


Fig. 4: Distribution of the predicted bounding boxes on different IoU metrics. All results are calculated on the *val* set.

Comparison to one-stage and two-stage SOTAs. We first compare SimREC with SOTA methods specifically designed for REC, of which results are given in Tab. IV and Tab. VI. For a fair comparison, we remove VG augmentations when compared to these models. Other training details, such as data augmentation, are also remain comparable with newly proposed REC models [42], [45]. From this table, we can see that SimREC outperforms all these methods, *e.g.*, +1.51%, +2.47% and +4.01% on three datasets, respectively. Besides, SimREC also have superior efficiency. With much better performance, SimREC further enhances the speed advantage against two-stage methods, *e.g.*, +21.4 times. Compared with one-stage SOTAs, SimREC is also much more lightweight and efficient, *i.e.*, +35.5 fps.

we also compare SimREC with existing pre-trained REC models. Under the similar setups, SimREC achieves better performance than MDETR [51] and UniTAB [70], *e.g.*, +4.02% on RefCOCOg. Compared to multi-task approaches [42], [47], [48], which requires additional labeled data, SimREC also demonstrates comparable results and significant efficiency. For instance, SimREC achieves similar performance to PolyFormer-L on RefCOCO with 22 times faster inference speed. These results greatly confirm that SimREC achieves the better trade-offs between performance and efficiency than existing methods.

Comparison with large-scale BERT-style pre-trained models. We compare SimREC with a set of large-scale BERT-style pre-trained models in Tab. V, which includes ViLBert [23], ERNIE-ViL [26], UNITER [24] and VILLA [25]. These methods all apply the expensive BERT-style pre-training with

millions of vision-language examples [19], [52], [84], [85], and they are also fine-tuned on REC datasets. From Tab. V, we surprisingly observe that our simple yet lightweight model can outperform these large models on all benchmark datasets. Compared to VILLA-L [25], the performance gains of SimREC can be up to +11.22% on RefCOCO *testB*, and the inference time is also reduced by 23 times. Even compared to the recently proposed multi-task model, *i.e.*, OFA [49], SimREC also has comparable performance and better efficiency. More importantly, the parameter size and training overhead of SimREC are all far less than these methods.

Since these large models have dominated various V&L tasks [21], [52], these results actually confirm that one-stage REC can be a “survivor” in the era dominated by large BERT-style pre-trained models. From the experiments, we find that one-stage REC is an efficient way for learning vision-and-language alignment. Thus, SimREC can obtain superior performance than the pre-trained models with much fewer training examples. Meanwhile, the objective of most BERT-style pre-trained models is based on region-text matching and their structures are also modular. In this case, their performance upper-bounds are prone to be limited by the independent visual backbones like Faster RCNN [63].

3) *Generalization to Transformer-based REC model:* To validate the generalization ability of SimREC framework, we apply our findings to Transformer-based models, *i.e.*, ViLT [83] and TransVG [9], of which results are given in Tab. VII. From these results, the first observation is that our findings can significantly improve the performance of ViLT [83] on REC, *e.g.*, +8.94% on RefCOCO+ *testB*. Be-

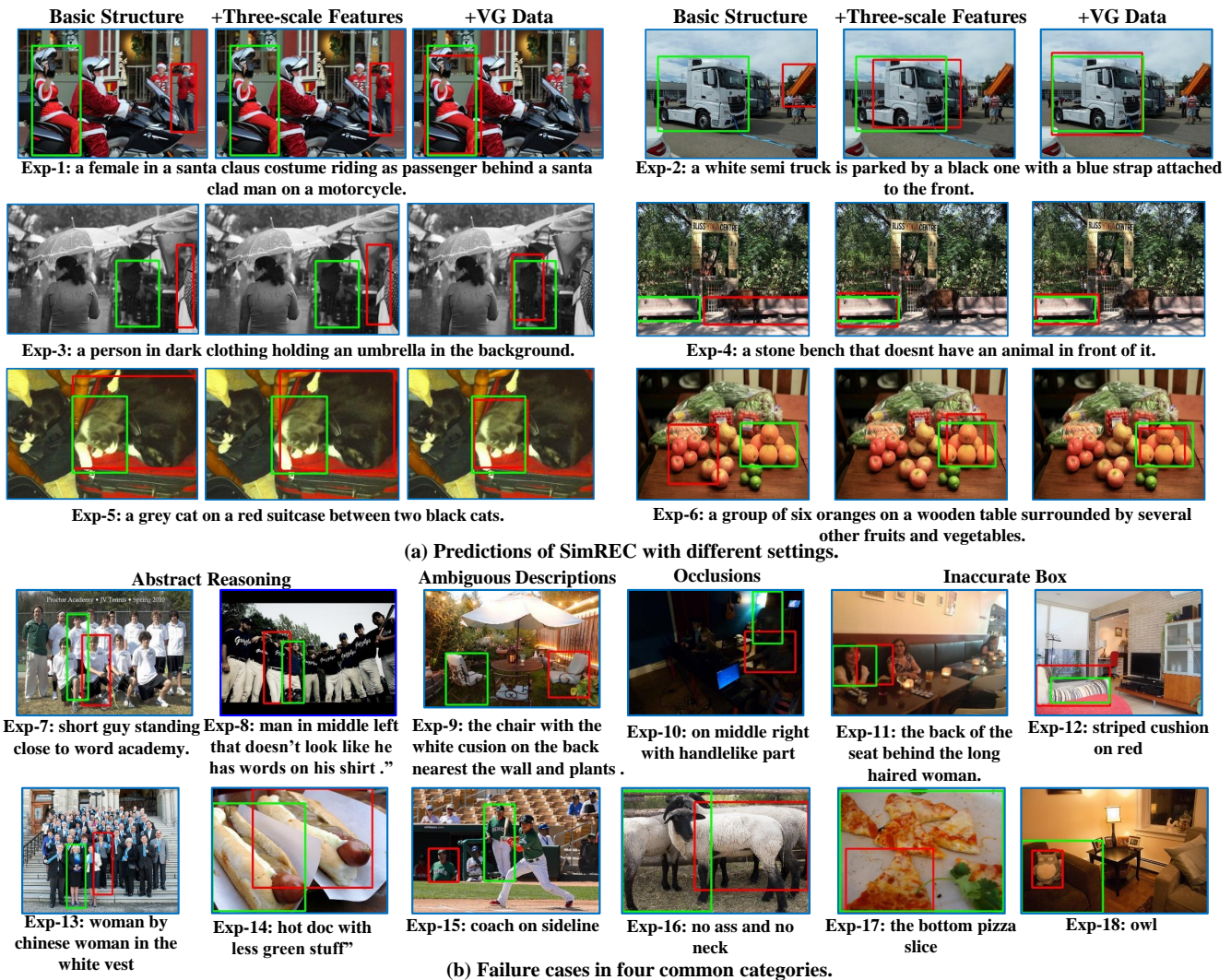


Fig. 5: Visualizations of predictions by SimREC with different settings and failure cases. The box of green color is the ground-truth, and the one of red is the prediction.

sides, we also find that the performance gains are more obvious on complex expressions and descriptions about objects. For example, the performances gains are +3.09% on RefCOCO testA, which are improved to +7.7% on RefCOCOg test. However, SimREC still outperforms these models on three datasets, greatly confirming the simple and lightweight structure of SimREC. Overall, these results greatly validate the generalization ability of our findings on Transformer-based model.

4) *Qualitative Analysis.*: In Fig. 5, we visualize the predictions by SimREC with different settings, and also give some typical failure cases.

From Fig. 5.(a), we can observe that without multi-scale features and data augmentation, SimREC is easy to fail to understand the expression containing various attributes or relationships. The adoption of multi-scale features and data augmentation can obviously help the model in visual concept understanding as well as relational reasoning. Fig. 5.(b) lists the common failure detections in the well-improved SimREC. Some of them are attributed to the label noisy, *e.g.*, the 9-*th* and 15-*th* examples, while some are too abstract or beyond the ability of REC. For instance, the 7-*th* example requires the

model to understand the characters in the image. Meanwhile, the object occlusions also cause the failure of detection, *e.g.*, the 10-*th* example. Besides, we observe that some failure cases are attributed to the inaccurate regression. For example, SimREC well locates the target object in the 11-*th* and 12-*th* example, but fails in accurately regressing the bounding box of the referent. These examples confirm the effectiveness of our findings, and also demonstrate the upper bound of SimREC.

V. CONCLUSION

In this paper, we present an empirical study for one-stage REC, which ablates 42 candidate designs/settings via over 100 experimental trails. This study not only yields the key factors for one-stage REC in addition to multi-modal fusion, but also reflects some findings against common impressions about REC. By combing the empirical findings, we also improve the simple REC network (SimREC) by a large margin, which greatly outperforms existing REC models in both accuracy and efficiency. More importantly, SimREC have better performance than a set of large-scale pre-trained V&L models with much less training overhead and parameters. We believe that

the findings of this paper can provide useful references for the development of REC, and also give some inspirations for the V&L research.

ACKNOWLEDGMENT

This work was supported by National Key R&D Program of China (No.2022ZD0118201), the National Science Fund for Distinguished Young Scholars (No.62025603), the National Natural Science Foundation of China (No. U21B2037, No. U22B2051, No. 62176222, No. 62176223, No. 62176226, No. 62072386, No. 62072387, No. 62072389, No. 62002305 and No. 62272401), and the Natural Science Foundation of Fujian Province of China (No.2021J01002, No.2022J06001), the China Fundamental Research Funds for the Central Universities (Grant No. 20720220068) and the Major Key Project of PCL (PCL2021A13).

REFERENCES

- [1] Y. Zhou, R. Ji, G. Luo, X. Sun, J. Su, X. Ding, C.-W. Lin, and Q. Tian, "A real-time global inference network for one-stage referring expression comprehension," *IEEE Transactions on Neural Networks and Learning Systems*, 2021.
- [2] G. Luo, Y. Zhou, X. Sun, L. Cao, C. Wu, C. Deng, and R. Ji, "Multi-task collaborative network for joint referring expression comprehension and segmentation," in *Proceedings of the IEEE/CVF Conference on Computer Vision and Pattern Recognition*, 2020, pp. 10 034–10 043.
- [3] L. Yu, Z. Lin, X. Shen, J. Yang, X. Lu, M. Bansal, and T. L. Berg, "Mattnet: Modular attention network for referring expression comprehension," in *CVPR*, 2018.
- [4] M. Sun, J. Xiao, and E. G. Lim, "Iterative shrinking for referring expression grounding using deep reinforcement learning," in *Proceedings of the IEEE/CVF Conference on Computer Vision and Pattern Recognition*, 2021, pp. 14 060–14 069.
- [5] P. Wang, Q. Wu, J. Cao, C. Shen, L. Gao, and A. v. d. Hengel, "Neighbourhood watch: Referring expression comprehension via language-guided graph attention networks," in *CVPR*, 2019.
- [6] D. Liu, H. Zhang, F. Wu, and Z.-J. Zha, "Learning to assemble neural module tree networks for visual grounding," in *ICCV*, 2019.
- [7] Z. Yang, B. Gong, L. Wang, W. Huang, D. Yu, and J. Luo, "A fast and accurate one-stage approach to visual grounding," in *ICCV*, 2019.
- [8] Z. Yang, T. Chen, L. Wang, and J. Luo, "Improving one-stage visual grounding by recursive sub-query construction," *arXiv preprint arXiv:2008.01059*, 2020.
- [9] J. Deng, Z. Yang, T. Chen, W. Zhou, and H. Li, "Transvg: End-to-end visual grounding with transformers," *arXiv preprint arXiv:2104.08541*, 2021.
- [10] L. Yu, P. Poirson, S. Yang, A. C. Berg, and T. L. Berg, "Modeling context in referring expressions," in *European Conference on Computer Vision*. Springer, 2016, pp. 69–85.
- [11] M. Bajaj, L. Wang, and L. Sigal, "G3raphground: Graph-based language grounding," in *Proceedings of the IEEE/CVF International Conference on Computer Vision*, 2019, pp. 4281–4290.
- [12] X. Liu, Z. Wang, J. Shao, X. Wang, and H. Li, "Improving referring expression grounding with cross-modal attention-guided erasing," in *Proceedings of the IEEE/CVF Conference on Computer Vision and Pattern Recognition*, 2019, pp. 1950–1959.
- [13] B. Huang, D. Lian, W. Luo, and S. Gao, "Look before you leap: Learning landmark features for one-stage visual grounding," in *Proceedings of the IEEE/CVF Conference on Computer Vision and Pattern Recognition*, 2021, pp. 16 888–16 897.
- [14] V. K. Nagaraja, V. I. Morariu, and L. S. Davis, "Modeling context between objects for referring expression understanding," in *ECCV*, 2016.
- [15] Z. Zhong, L. Zheng, G. Kang, S. Li, and Y. Yang, "Random erasing data augmentation," in *Proceedings of the AAAI Conference on Artificial Intelligence*, vol. 34, no. 07, 2020, pp. 13 001–13 008.
- [16] E. D. Cubuk, B. Zoph, J. Shlens, and Q. V. Le, "Randaugmt: Practical automated data augmentation with a reduced search space," in *Proceedings of the IEEE/CVF Conference on Computer Vision and Pattern Recognition Workshops*, 2020, pp. 702–703.
- [17] S. Yun, D. Han, S. J. Oh, S. Chun, J. Choe, and Y. Yoo, "Cutmix: Regularization strategy to train strong classifiers with localizable features," in *Proceedings of the IEEE/CVF International Conference on Computer Vision*, 2019, pp. 6023–6032.
- [18] T. DeVries and G. W. Taylor, "Improved regularization of convolutional neural networks with cutout," *arXiv preprint arXiv:1708.04552*, 2017.
- [19] R. Krishna, Y. Zhu, O. Groth, J. Johnson, K. Hata, J. Kravitz, S. Chen, Y. Kalantidis, L.-J. Li, D. A. Shamma *et al.*, "Visual genome: Connecting language and vision using crowdsourced dense image annotations," in *arXiv preprint*, 2016.
- [20] S. Antol, A. Agrawal, J. Lu, M. Mitchell, D. Batra, C. L. Zitnick, and D. Parikh, "Vqa: Visual question answering," in *ICCV*, 2015.
- [21] H. Xu and K. Saenko, "Ask, attend and answer: Exploring question-guided spatial attention for visual question answering," in *ECCV*, 2016.
- [22] Y. Zhou, R. Ji, X. Sun, J. Su, D. Meng, Y. Gao, and C. Shen, "Plenty is plague: Fine-grained learning for visual question answering," *IEEE transactions on pattern analysis and machine intelligence*, 2019.
- [23] J. Lu, D. Batra, D. Parikh, and S. Lee, "Vilbert: Pretraining task-agnostic visiolinguistic representations for vision-and-language tasks," *arXiv preprint arXiv:1908.02265*, 2019.
- [24] Y.-C. Chen, L. Li, L. Yu, A. El Kholly, F. Ahmed, Z. Gan, Y. Cheng, and J. Liu, "Uniter: Universal image-text representation learning," in *European conference on computer vision*. Springer, 2020, pp. 104–120.
- [25] Z. Gan, Y.-C. Chen, L. Li, C. Zhu, Y. Cheng, and J. Liu, "Large-scale adversarial training for vision-and-language representation learning," in *NeurIPS*, 2020.
- [26] F. Yu, J. Tang, W. Yin, Y. Sun, H. Tian, H. Wu, and H. Wang, "Ernie-vil: Knowledge enhanced vision-language representations through scene graphs," in *Proceedings of the AAAI Conference on Artificial Intelligence*, vol. 35, no. 4, 2021, pp. 3208–3216.
- [27] R. Hu, M. Rohrbach, J. Andreas, T. Darrell, and K. Saenko, "Modeling relationships in referential expressions with compositional modular networks," in *CVPR*, 2017.
- [28] R. Hu, H. Xu, M. Rohrbach, J. Feng, K. Saenko, and T. Darrell, "Natural language object retrieval," in *CVPR*, 2016.
- [29] J. Liu, L. Wang, and M. Yang, "Referring expression generation and comprehension via attributes," in *ICCV*, 2017.
- [30] R. Luo and G. Shakhnarovich, "Comprehension-guided referring expressions," in *CVPR*, 2017.
- [31] L. Yu, P. Poirson, S. Yang, A. C. Berg, and T. L. Berg, "Modeling context in referring expressions," in *ECCV*, 2016.
- [32] L. Yu, H. Tan, M. Bansal, and T. L. Berg, "A joint speaker-listener-reinforcer model for referring expressions," in *CVPR*, 2017.
- [33] Y. Zhang, L. Yuan, Y. Guo, Z. He, I. Huang, and H. Lee, "Discriminative bimodal networks for visual localization and detection with natural language queries," in *CVPR*, 2017.
- [34] L. Yu, Z. Lin, X. Shen, J. Yang, X. Lu, M. Bansal, and T. L. Berg, "Mattnet: Modular attention network for referring expression comprehension," in *CVPR*, 2018.
- [35] Y. Bu, L. Li, J. Xie, Q. Liu, Y. Cai, Q. Huang, and Q. Li, "Scene-text oriented referring expression comprehension," *IEEE Transactions on Multimedia*, 2022.
- [36] M. Sun, W. Suo, P. Wang, Y. Zhang, and Q. Wu, "A proposal-free one-stage framework for referring expression comprehension and generation via dense cross-attention," *IEEE Transactions on Multimedia*, 2022.
- [37] Y. Qiao, C. Deng, and Q. Wu, "Referring expression comprehension: A survey of methods and datasets," *IEEE Transactions on Multimedia*, vol. 23, pp. 4426–4440, 2020.
- [38] G. Luo, Y. Zhou, X. Sun, Y. Wang, L. Cao, Y. Wu, F. Huang, and R. Ji, "Towards lightweight transformer via group-wise transformation for vision-and-language tasks," *IEEE Transactions on Image Processing*, vol. 31, pp. 3386–3398, 2022.
- [39] G. Luo, Y. Zhou, X. Sun, X. Ding, Y. Wu, F. Huang, Y. Gao, and R. Ji, "Towards language-guided visual recognition via dynamic convolutions," *arXiv preprint arXiv:2110.08797*, 2021.
- [40] Y. Zhou, T. Ren, C. Zhu, X. Sun, J. Liu, X. Ding, M. Xu, and R. Ji, "Trar: Routing the attention spans in transformer for visual question answering," in *Proceedings of the IEEE/CVF International Conference on Computer Vision*, 2021, pp. 2074–2084.
- [41] A. Sadhu, K. Chen, and R. Nevatia, "Zero-shot grounding of objects from natural language queries," in *Proceedings of the IEEE/CVF International Conference on Computer Vision*, 2019, pp. 4694–4703.
- [42] C. Zhu, Y. Zhou, Y. Shen, G. Luo, X. Pan, M. Lin, C. Chen, L. Cao, X. Sun, and R. Ji, "Seqtr: A simple yet universal network for visual grounding," in *Computer Vision–ECCV 2022: 17th European Confer-*

- ence, Tel Aviv, Israel, October 23–27, 2022, *Proceedings, Part XXXV*. Springer, 2022, pp. 598–615.
- [43] Y. Liao, A. Zhang, Z. Chen, T. Hui, and S. Liu, “Progressive language-customized visual feature learning for one-stage visual grounding,” *IEEE Transactions on Image Processing*, vol. 31, pp. 4266–4277, 2022.
- [44] H. Zhao, J. T. Zhou, and Y.-S. Ong, “Word2pix: Word to pixel cross-attention transformer in visual grounding,” *IEEE Transactions on Neural Networks and Learning Systems*, 2022.
- [45] J. Ye, J. Tian, M. Yan, X. Yang, X. Wang, J. Zhang, L. He, and X. Lin, “Shifting more attention to visual backbone: Query-modulated refinement networks for end-to-end visual grounding,” in *Proceedings of the IEEE/CVF Conference on Computer Vision and Pattern Recognition*, 2022, pp. 15 502–15 512.
- [46] A. Vaswani, N. Shazeer, N. Parmar, J. Uszkoreit, L. Jones, A. N. Gomez, L. Kaiser, and I. Polosukhin, “Attention is all you need,” in *NIPS*, 2017.
- [47] J. Liu, H. Ding, Z. Cai, Y. Zhang, R. K. Satzoda, V. Mahadevan, and R. Manmatha, “Polyformer: Referring image segmentation as sequential polygon generation,” in *Proceedings of the IEEE/CVF Conference on Computer Vision and Pattern Recognition*, 2023, pp. 18 653–18 663.
- [48] B. Yan, Y. Jiang, J. Wu, D. Wang, P. Luo, Z. Yuan, and H. Lu, “Universal instance perception as object discovery and retrieval,” in *Proceedings of the IEEE/CVF Conference on Computer Vision and Pattern Recognition*, 2023, pp. 15 325–15 336.
- [49] P. Wang, A. Yang, R. Men, J. Lin, S. Bai, Z. Li, J. Ma, C. Zhou, J. Zhou, and H. Yang, “Ofa: Unifying architectures, tasks, and modalities through a simple sequence-to-sequence learning framework,” in *International Conference on Machine Learning*. PMLR, 2022, pp. 23 318–23 340.
- [50] Z. Zhang, Z. Wei, Z. Huang, R. Niu, and P. Wang, “One for all: One-stage referring expression comprehension with dynamic reasoning,” *Neurocomputing*, vol. 518, pp. 523–532, 2023.
- [51] A. Kamath, M. Singh, Y. LeCun, G. Synnaeve, I. Misra, and N. Carion, “Mdetr-modulated detection for end-to-end multi-modal understanding,” in *Proceedings of the IEEE/CVF International Conference on Computer Vision*, 2021, pp. 1780–1790.
- [52] T. Lin, M. Maire, S. J. Belongie, J. Hays, P. Perona, D. Ramanan, P. Dollár, and C. L. Zitnick, “Microsoft coco: Common objects in context,” in *ECCV*, 2014.
- [53] J. Devlin, M. Chang, K. Lee, and K. Toutanova, “Bert: Pre-training of deep bidirectional transformers for language understanding,” in *arXiv preprint*, 2018.
- [54] Z. Yu, J. Yu, Y. Cui, D. Tao, and Q. Tian, “Deep modular co-attention networks for visual question answering,” in *Proceedings of the IEEE/CVF Conference on Computer Vision and Pattern Recognition*, 2019, pp. 6281–6290.
- [55] V. Nair and G. E. Hinton, “Rectified linear units improve restricted boltzmann machines,” in *Icml*, 2010.
- [56] J. Redmon and A. Farhadi, “Yolov3: An incremental improvement,” in *arXiv preprint*, 2018.
- [57] K. Simonyan and A. Zisserman, “Very deep convolutional networks for large-scale image recognition,” in *ICLR*, 2015.
- [58] C.-Y. Wang, H.-Y. M. Liao, Y.-H. Wu, P.-Y. Chen, J.-W. Hsieh, and I.-H. Yeh, “Cspnet: A new backbone that can enhance learning capability of cnn,” in *Proceedings of the IEEE/CVF conference on computer vision and pattern recognition workshops*, 2020, pp. 390–391.
- [59] S. Hochreiter and J. Schmidhuber, “Long short-term memory,” in *Neural computation*, 1997.
- [60] J. Pennington, R. Socher, and C. Manning, “Glove: Global vectors for word representation,” in *EMNLP*, 2014.
- [61] Z. Ge, S. Liu, F. Wang, Z. Li, and J. Sun, “Yolox: Exceeding yolo series in 2021,” *arXiv preprint arXiv:2107.08430*, 2021.
- [62] H. Rezatofghi, N. Tsoi, J. Gwak, A. Sadeghian, I. Reid, and S. Savarese, “Generalized intersection over union: A metric and a loss for bounding box regression,” in *Proceedings of the IEEE/CVF Conference on Computer Vision and Pattern Recognition*, 2019, pp. 658–666.
- [63] S. Ren, K. He, R. Girshick, and J. Sun, “Faster r-cnn: towards real-time object detection with region proposal networks,” in *TPAMI*, 2017.
- [64] T.-Y. Lin, P. Goyal, R. Girshick, K. He, and P. Dollár, “Focal loss for dense object detection,” in *Proceedings of the IEEE international conference on computer vision*, 2017, pp. 2980–2988.
- [65] H. Zhang, M. Cisse, Y. N. Dauphin, and D. Lopez-Paz, “mixup: Beyond empirical risk minimization,” *arXiv preprint arXiv:1710.09412*, 2017.
- [66] T. He, Z. Zhang, H. Zhang, Z. Zhang, J. Xie, and M. Li, “Bag of tricks for image classification with convolutional neural networks,” in *Proceedings of the IEEE/CVF Conference on Computer Vision and Pattern Recognition*, 2019, pp. 558–567.
- [67] A. Tarvainen and H. Valpola, “Mean teachers are better role models: Weight-averaged consistency targets improve semi-supervised deep learning results,” *arXiv preprint arXiv:1703.01780*, 2017.
- [68] Z. Liu, Y. Lin, Y. Cao, H. Hu, Y. Wei, Z. Zhang, S. Lin, and B. Guo, “Swin transformer: Hierarchical vision transformer using shifted windows,” in *Proceedings of the IEEE/CVF international conference on computer vision*, 2021, pp. 10 012–10 022.
- [69] A. Dosovitskiy, L. Beyer, A. Kolesnikov, D. Weissenborn, X. Zhai, T. Unterthiner, M. Dehghani, M. Minderer, G. Heigold, S. Gelly *et al.*, “An image is worth 16x16 words: Transformers for image recognition at scale,” *arXiv preprint arXiv:2010.11929*, 2020.
- [70] Z. Yang, Z. Gan, J. Wang, X. Hu, F. Ahmed, Z. Liu, Y. Lu, and L. Wang, “Unitab: Unifying text and box outputs for grounded vision-language modeling,” in *European Conference on Computer Vision*. Springer, 2022, pp. 521–539.
- [71] L. Wang, Y. Li, J. Huang, and S. Lazebnik, “Learning two-branch neural networks for image-text matching tasks,” *IEEE Transactions on Pattern Analysis and Machine Intelligence*, vol. 41, no. 2, pp. 394–407, 2018.
- [72] Z. Yu, J. Yu, C. Xiang, Z. Zhao, Q. Tian, and D. Tao, “Rethinking diversified and discriminative proposal generation for visual grounding,” *arXiv preprint arXiv:1805.03508*, 2018.
- [73] A. Sadhu, K. Chen, and R. Nevatia, “Zero-shot grounding of objects from natural language queries,” in *ICCV*, 2019.
- [74] J. Mao, J. Huang, A. Toshev, O. M. Camburu, A. L. Yuille, and K. P. Murphy, “Generation and comprehension of unambiguous object descriptions,” in *CVPR*, 2016.
- [75] J. C. Duchi, E. Hazan, and Y. Singer, “Adaptive subgradient methods for online learning and stochastic optimization,” in *JMLR*, 2011.
- [76] R. Krishna, Y. Zhu, O. Groth, J. Johnson, K. Hata, J. Kravitz, S. Chen, Y. Kalantidis, L.-J. Li, D. A. Shamma *et al.*, “Visual genome: Connecting language and vision using crowdsourced dense image annotations,” *International journal of computer vision*, vol. 123, no. 1, pp. 32–73, 2017.
- [77] H. Jiang, I. Misra, M. Rohrbach, E. Learned-Miller, and X. Chen, “In defense of grid features for visual question answering,” in *Proceedings of the IEEE/CVF Conference on Computer Vision and Pattern Recognition*, 2020, pp. 10 267–10 276.
- [78] G. Luo, Y. Zhou, R. Ji, X. Sun, J. Su, C.-W. Lin, and Q. Tian, “Cascade grouped attention network for referring expression segmentation,” in *Proceedings of the 28th ACM International Conference on Multimedia*, 2020, pp. 1274–1282.
- [79] Z. Zhang, T. He, H. Zhang, Z. Zhang, J. Xie, and M. Li, “Bag of freebies for training object detection neural networks,” *arXiv preprint arXiv:1902.04103*, 2019.
- [80] P. Anderson, X. He, C. Buehler, D. Teney, M. Johnson, S. Gould, and L. Zhang, “Bottom-up and top-down attention for image captioning and visual question answering,” in *CVPR*, 2018.
- [81] Z. Lan, M. Chen, S. Goodman, K. Gimpel, P. Sharma, and R. Soricut, “Albert: A lite bert for self-supervised learning of language representations,” *arXiv preprint arXiv:1909.11942*, 2019.
- [82] R. Kiros, R. Salakhutdinov, and R. S. Zemel, “Multimodal neural language models,” in *ICML*, 2014.
- [83] W. Kim, B. Son, and I. Kim, “Vilt: Vision-and-language transformer without convolution or region supervision,” *arXiv preprint arXiv:2102.03334*, 2021.
- [84] P. Sharma, N. Ding, S. Goodman, and R. Soricut, “Conceptual captions: A cleaned, hypernymed, image alt-text dataset for automatic image captioning,” in *Proceedings of the 56th Annual Meeting of the Association for Computational Linguistics (Volume 1: Long Papers)*, 2018, pp. 2556–2565.
- [85] V. Ordonez, G. Kulkarni, and T. Berg, “Im2text: Describing images using 1 million captioned photographs,” *Advances in neural information processing systems*, vol. 24, pp. 1143–1151, 2011.



Gen Luo is currently pursuing the phd's degree in Xiamen University. His research interests include vision-and-language learning.



Rongrong Ji (Senior Member, IEEE) is a Nanqiang Distinguished Professor at Xiamen University, the Deputy Director of the Office of Science and Technology at Xiamen University, and the Director of Media Analytics and Computing Lab. He was awarded as the National Science Foundation for Excellent Young Scholars (2014), the National Ten Thousand Plan for Young Top Talents (2017), and the National Science Foundation for Distinguished Young Scholars (2020). His research falls in the field of computer vision, multimedia analysis, and machine learning. He has published 50+ papers in ACM/IEEE Transactions, including TPAMI and IJCV, and 100+ full papers on top-tier conferences, such as CVPR and NeurIPS. His publications have got over 10K citations in Google Scholar. He was the recipient of the Best Paper Award of ACM Multimedia 2011. He has served as Area Chairs in top-tier conferences such as CVPR and ACM Multimedia. He is also an Advisory Member for Artificial Intelligence Construction in the Electronic Information Education Committee of the National Ministry of Education.



Yiyi Zhou received the Ph.D. degree from Xiamen University, China, in 2019, under the supervision of Prof. Rongrong Ji. He was a Postdoctoral Research Search Fellow with Xiamen University from 2019 to 2022. He is currently an associate professor at School of Informatics and Institute of Artificial Intelligence of Xiamen University. His research interests include multimedia analysis and computer vision.



Jiamu Sun received his Bachelor Degree from Hebei University of Technology, China, in 2021. He is a postgraduate student supervised by Prof. Rongrong Ji in Media Analytics and Computing (MAC) lab of Xiamen University, China.



Xiaoshuai Sun (Senior Member, IEEE) received the B.S. degree in computer science from Harbin Engineering University, Harbin, China, in 2007, and the M.S. and Ph.D. degrees in computer science and technology from the Harbin Institute of Technology, Harbin, in 2009 and 2015, respectively. He was a Postdoctoral Research Fellow with the University of Queensland from 2015 to 2016. He served as a Lecturer with the Harbin Institute of Technology from 2016 to 2018. He is currently an Associate Professor with Xiamen University, China. He was a recipient of the Microsoft Research Asia Fellowship in 2011.